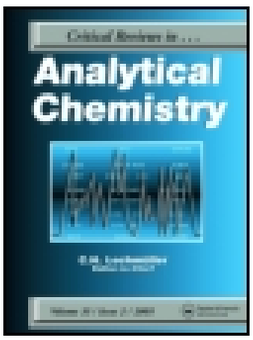

Critical Reviews in Analytical Chemistry

ISSN: 1040-8347 (Print) 1547-6510 (Online) Journal homepage: http://www.tandfonline.com/loi/batc20

Fiber-optic surface plasmon resonance based biosensor technique: Fabrication, advancement and application

Gaoling Liang, Zewei Luo, Kunping Liu, Yimin Wang, Jianxiong Dai & Yixiang Duan

To cite this article: Gaoling Liang, Zewei Luo, Kunping Liu, Yimin Wang, Jianxiong Dai & Yixiang Duan (2015): Fiber-optic surface plasmon resonance based biosensor technique: Fabrication, advancement and application, Critical Reviews in Analytical Chemistry, DOI: 10.1080/10408347.2015.1045119

To link to this article: http://dx.doi.org/10.1080/10408347.2015.1045119

Accepted author version posted online: 13 Nov 2015.

Fiber-optic surface plasmon resonance based biosensor technique: Fabrication, advancement and application

Gaoling Liang[a], Zewei Luo[b], Kunping Liu[a,c], Yimin Wang[b], Jianxiong Dai[d], and Yixiang Duan[b]*

[a]College of Chemistry, Sichuan University, Chengdu, China

[b]Research Center of Analytical Instrumentation, Key Laboratory of Bio-resource and Eco-environment, Ministry of Education, College of Life Science, Sichuan University, Chengdu, China

[c]Faculty of Biotechnology Industry, Chengdu University, Chengdu, China

[d]Analytical & Testing Center, Sichuan University, Chengdu, China

Address correspondence to Prof. Yixiang Duan, Research Center of Analytical Instrumentation, College of Life Science, Sichuan University, 29 Wangjiang Road, Chengdu 610064, China. E-mail: yduan@scu.edu.cn

Abstract

Fiber-optic based biosensors with surface plasmon resonance (SPR) technology are advanced label-free optical biosensing methods. They have brought tremendous advances in the sensing of various chemical and biological species. This review summarizes four sensing configurations (prism, grating, waveguide and fiber-optic) with two ways, attenuated total reflection (ATR) and diffraction to excite the surface plasmons. Meanwhile, the designs of different probes (U-bent, tapered and other probes) are also described. Finally, four major types

of biosensors: immunosensor, DNA biosensor, enzyme biosensor and living cell biosensor are discussed detailly from their sensing principles and applications. Future prospects of fiber-optic based SPR sensor technology are discussed.

Keywords

Surface plasmons, localized surface plasmon resonance (LSPR), probe geometry, fiber-optic biosensor

1. Introduction

The first report about the SPR biosensor was concerned with the sensing of gases in the early 1980s. Since then, the number of publications covering the SPR biosensors for detecting chemical and biological species has been growing rapidly. Great advances have been made for its technology and applications. Since the 1990's, SPR biosensing has become the main method of studying biomolecular interactions (Piliarik et al., 2009) because of its ability to detect the binding of analytes from a liquid sample to some biomolecular recognition elements immobilized on the surface of a sensor. The development of the fiber-optic sensor based on SPR is described in this review by going through the formation of SPR theory, followed by descriptions of prism SPR and of fiber-optic SPR. The use of the fiber-optic technique in SPR biosensing can be attributed to the fact that it can be used to tackle different measurement situations where conventional sensors are not effective. This technique has several important features: no electromagnetic interference, a simple optical set up, the capacity of performing remote sensing, real-time sensing and label free sensing. The fiber-optic SPR sensors meet the demands of time and space saving, low sample volume, low-cost, high sensitivity, portability and miniaturization. Therefore, these biosensors have been recently extensively investigated.

In this review, we begin with the fundamentals of surface plasmons and the principles of their optical generation. Two types of surface plasmon resonance, LSPR and propagating surface plasmon resonance (PSPR) are included. The biosensors are classified according to the nature of

the biological recognition element used for sensing: enzyme, antibody/antigen, nucleic acid, or living cell. The corresponding applications are presented. Incorporating fiber-optic technology with SPR sensing schema provides an effective, compact, and label-free biosensing method when compared to conventional biosensors. Thus, given its importance in research, there is a need to provide a separate review of the fiber-optic SPR biosensor.

2. Principles

2.1. Fundamentals of fiber-optics

Optical fibers consist of a cylindrical core and a surrounding cladding, both of which are made of silica. The core is generally doped with germanium to make its refractive index slightly higher than the cladding refractive index (Leung et al., 2007). Since the light is transmitted in the optical fibers by total internal reflection (TIR), the refractive index of the core (n_1) must be larger than that of the cladding (n_2). In order to meet the condition of TIR, the angle of incidence must be larger than the critical angle defined by Snell's law ($\theta c=\sin^{-1}[n_2/n_1]$) (Marazuela and Moreno-Bondi, 2002). When the incident light strikes the interface of the core and cladding, the reflected light doesn't directly appear (Gupta and Verma, 2009). A small portion of the light penetrates the optically thinner medium to a depth of about one wavelength and propagates along the boundary for a distance of approximately half of the light wavelength. Then the light returns to the optically denser medium. The field in the lower refractive index medium is called the evanescent field and the wave corresponding to it is called the evanescent wave (EW). The

intensity of the EW's electromagnetic field has a maximum value at the interface, while exponentially decaying with the perpendicular distance to the interface. The distance to which the evanescent field extends beyond the core-cladding boundary is referred as the penetration depth. Its value is in the range required for the electric field amplitude to fall to 1/e (0.37) of its value at the core–cladding interface. The electric field can be described as: $E_{(X)} = E_0 \exp(\frac{-x}{d_p})$ where x is the distance from the fiber core (x = 0 at the core-cladding interface), E_0 is the magnitude of the field at the interface, and d_p is the penetration depth. The penetration depth is given by $d_p = \frac{\lambda}{2\pi\sqrt{n^2_{co}\sin^2\theta - n^2_{cl}}}$ where λ is the wavelength of the light source, θ is the angle of incidence of the light at the core/cladding interface, and n_{co} and n_{cl} are the refractive indices (RI) of the core and cladding, respectively. We can see from this formula that the intrinsic characteristics of the optical fiber (n_{co} and n_{cl}) will influence the d_p, which is also a function of the wavelength of the light and the angle of incidence (Marazuela and Moreno-Bondi, 2002).

2.2. Surface plasmons and localized surface plasmons

A surface plasmon, sometimes called a surface plasmon polarization or a surface plasma wave (SPW), is a transverse magnetically (TM) or a p-polarized light wave. This wave is longitudinal and has a magnetic vector vertical to the plane of incidence. The magnetic vector travels along the upper surface of the metal film. Moreover, the electromagnetic field is distributed as follows. At the interface, the intensity of the field is strongest and diminishes

exponentially into both materials with a decay depth on the order of about a light wavelength. The major part of the field is located in the dielectric (Guo, 2012).

There are two types of surface plasmons, propagating surface plasmons (in the planar surface) and localized surface plasmons (in the metallic nanostructures), as shown in Fig.1. Propagating surface plasmons are charge density oscillations at the interface of the metal film and the dielectric (See Fig.1a). At the surface of planar metal layer, the plasmon oscillation is optically excited. There is an equal positively charged ion lattice in the metal. When the metal feels the interference of the electromagnetic field, the distribution of the electromagnetic field density will not be homogeneous. When the density of the free electrons is less than the average electron density in a given volume, the movement of free electrons will take place. That is, the negatively charged free electrons begin to get attracted to the positively charged ion background. These electrons which are attracted will obtain additional momentum and accumulate with a density greater than necessary for charge neutrality, which results in an excess negative electrical charge. Coulombic repulsion among the free electrons forces them to leave. Therefore, an oscillation of the valence electrons relative to the positively charged background is formed. Due to the field effect of the coulombic force, a collective electron density oscillation is established. Because of this plasma oscillation, an electromagnetic surface wave is generated (See Fig.1a). The quantum of the plasma oscillation is called a plasmon. These plasmons are generated by the collective oscillation of the electrons surrounding the atomic lattice sites of the metal in question.

As shown in Fig.1b, localized surface plasmons are similar to the propagating surface plasmons in how they are produced. However, the collective oscillations of the free electron cloud are in the metal nanoparticles rather than arising from the vibration of the conduction electrons in the plane of the metal film (Srivastava et al., 2009). In localized surface plasmons case, the light scatters from a topological defect on the surface of the metallic particles or nanostructures. The external electricfield of light cause the displacement of the electron gas with respect to the fixed ionic cores.

2.3. SPR and LSPR

SPR can be used as a label-free and highly sensitive optical analytical method. SPR can be excited by light or by electricity. It is known that surface plasmons are transverse magnetically waves, so a TM or p-polarized light can excite them under the resonance condition, that is, when the wave vector of the incident light matches the collective oscillation frequency of the surface electrons in the metal film. When SPR occurs, the interaction of the necessary light with the free electrons traps the light waves on the surface. This trapping results in the energy of the light transferring to the free electrons (Homola et al., 2008; Abdulhalim et al., 2008), which, in turn, is responsible for a dip in reflectance at the specific wavelength and at the appropriate angle.

LSPR is a well-studied nanoscale phenomenon similar to SPR (Srivastava et al., 2009). LSPR occurs when surface plasmons are confined in nanoparticles and localized optic modes, called localized surface plasmons, are observed. In the past decades, using LSPR technique in

sensing applications has generated considerable interest. The metal nanoparticles exhibit a strong absorption band in the UV-Vis region, which is not present in the bulk metal layer. The particle's optical excitation has a maximum value at the plasmon resonance frequency, which occurs at visible wavelengths for noble metal nanoparticles.

Table 1, shows a brief comparison of SPR and LSPR (Mayer and Hafner., 2011). Some experiments also have shown that the sensitivity of SPR is higher than that of LSPR, while LSPR has a better linearity (Yonzon et al., 2004; Zhao et al., 2006; Svedendahl et al., 2009; Chen and Ming, 2012). Both in SPR and LSPR, the most commonly used metals are silver and gold because of their unique optic properties and their absorption band, which is in the visible region. Silver has a narrower resonance curve and therefore it gives a higher signal-to-noise ratio (SNR). However, the disadvantage of Ag is its chemical reactivity (Leung et al., 2007). Therefore, gold is more usually used in sensing applications.

3. SPR sensing configurations

In order to excite the surface plasmon by light, the wave-vector of the excitation light must be equal to that of the surface plasmons. The propagation constant of an SPW is given by the following expression:

$$k_{sp} = \frac{\omega}{c}\left(\frac{\varepsilon_m \varepsilon_d}{\varepsilon_m + \varepsilon_d}\right) \quad (1)$$

Where ω represents the angular frequency, c represents the speed of light in a vacuum, and ε_m and ε_d are the dielectric constants of the metal and the dielectric, respectively. The propagation

constant of the light wave in the dielectric medium is described in Eq. (2):

$$k_s = \frac{\omega}{c}\sqrt{\varepsilon_s} \quad (2)$$

where ω represents the angular frequency, *c* represents the speed of light in a vacuum, and ε_s represents the dielectric constant of the dielectric medium. Since ε_m <0 and ε_s >0, for a given frequency, the propagation constant of a surface plasmon is greater than that of the light wave. Hence, light can't excite the surface plasmons at the metal-dielectric interface directly. In order to meet the resonance condition, the wave vector of the light must be increased. There are two basic methods used to achieve this increase, ATR and diffraction. Four couplers are used to modify the incident light: prism, waveguide, fiber-optic and grating. From the ray optics viewpoint, use of the first three structures is based on the ATR method, while the use of the fourth is based on diffraction.

3.1. Prism coupling

To allow optical excitation of surface plasmons, the light wave must be coupled to a surface plasmon at the interface. The momentum and the wave vector of the light are increased by passing the light wave through an optically denser medium, that is, a prism with high dielectric constant. In this case, the EW is the excitation light instead of the direct light. The EW and the SPW both spread along the boundary and exponentially decay into the dielectric medium. Consequently, interaction between the two waves is possible (Sharma et al., 2009). There are two prism configurations, the Otto configuration and the Kretschmann ATR method. See Fig. 2 and

Fig. 3.

As shown in Fig. 2, there is an air gap between the triangular prism base and the metal layer in the Otto-configuration. A light wave(p-polarized light) passes through a high refractive index prism and is totally reflected. Afterwards, an evanesent wave is generated and travels along the interface. Therefore, the evanescent field at the prism-air interface can excite the surface plasmons at the air-metal boundary. However, it is difficult to accurately control the air gap between the prism and the metal layer. Subsequently, Kretschmann found that if the metal layer is directly contacted with the prism, a significant improvement to the Otto configuration is obtained. In the Kretschmann configuration(See Fig. 3), there is no air gap between the triangular prism base and the metal layer. The prism and the metal layer are contacted directly, thus, this coupling configuration is more convinient. Under total reflection, an evanescent wave is generated which penetrates the thin metal film. The thickness of the metal film must be properly chosen typically around 50 nm. The EW excites the surface plasmon at the outer metal layer.

The fundamental necessity of optical excitation of a surface plasmon through a prism is that the propagation constant of the evanescent-wave is expressed by:

$$k_d = \frac{\omega}{c}\sqrt{\varepsilon_p}\sin\theta \qquad (3)$$

As is given in formula (3), the wave vector of the evanescent wave is related to the incident angle θ. Therefore the wave-vector of the evanescent wave is equal to that of the surface

plasmons through alternating the incident angle. The resonance condition is given by:

$$k_{sp} = \frac{\omega}{c}\left(\frac{\varepsilon_m \varepsilon_d}{\varepsilon_m + \varepsilon_d}\right) = k_d = \frac{\omega}{c}\sqrt{\varepsilon_p}\sin\theta \qquad (4)$$

in (3) and (4), where k_{sp} is the propagation constant of the surface plasmon, k_d is the propagation constant of the evanescent-wave, and θ represents the incident angle.

3.2. Grating coupling

As shown in Fig. 4, when the light impinging on the metal-dilectric interface at the incidence angle of θ, the momentum of the incident optical wave can also be enhanced by diffraction in a grating coupler. The original x-component of the wave vector of the incident photons k_x is increased by G through m = +1 diffraction order to match that of the surface plasmons (Wijaya et al., 2011).

In this method, given a light wave that is incident on a metallic grating, the wave vector of the incident light is increased to match the wave vector of the associated surface plasmons. Since the diffraction grating scatters the incident light wave, the propagation constant of the diffracted light is modified by an integer multiple of the grating wave number G. The resonance condition is accomplished by the diffraction order. Then the diffracted light excites the surface plasmons. The coupling condition by the metallic grating is described as:

$$k_d = k_x + mG = \frac{2\pi}{\lambda} n_d \sin\theta + m\frac{2\pi}{\Lambda} \qquad (5)$$

where k_d is the propagation constant of the diffracted light, k_x is the propagation constant of the incident light, G is the wavenumber of the grating, m=0, ± 1, $\pm 2\ldots$ is the diffraction order,

Λ is the grating period, and n_d represents the dielectric refractive index.

3.3. Waveguide coupling

For waveguide coupling method, the light propagates along the dielectric waveguide through TIR too. The propagated light takes the form of guided mode. A portion of the electromagnetic field of a guided mode propagated as an evanescent wave. When the light enters the region covered by the thin metal film, the evanescent field penetrates through the film to generate the SPR at the resonance condition. (Fig. 5)(Wijaya et al., 2011). When SPR phenomenon occurs, there is a dip in the transmitted spectrum. Thus, the intensity of the guided light wave in is different from the guided light wave out.

3.4. Fiber-optic coupling

The first work using optical fibers in SPR sensing was reported by Yee et al. in 1993 (Yee and Jorgenson, 1993). The traditional prism was replaced by a fiber-optic coupler. The various shortcomings of prism-based SPR sensing devices were: relatively bulky size, complex optics, complex mechanical structure, and the inability to be used for remote sensing. Fiber-optics overcame the problem of the prisms with the additional advantages of low sample volumes, portable set-up, and cost-effectiveness.

Fiber-optic waveguides are relatively simple structures (See Fig.6). The fundamental of exciting the surface plasmons is similar to prism coupling and to waveguide coupling based on ATR (Verma and Gupta, 2008). The core of an optical fiber is used to replace the prism, and the

evanescent wave is generated due to the ATR. The corresponding evanescent field excites the surface plasmons at the metal layer-dielectric sensing interface.

An optical fiber is a circular waveguide, which guides light based on the phenomenon of total internal reflection at the interface of the optical fiber core and the cladding surrounding the fiber core. There are two components of the light that propagate through an optical fiber. In the core is the guided field. In the cladding is the exponentially decaying evanescent field. When using the fiber-optic system in sensing, the light interacts with the fiber's surroundings. In a uniform-diameter fiber, the evanescent field decays to almost zero within the cladding. Therefore a uniform-diameter fiber is not suitable for sensing. One way to overcome the problem is to expose the evanescent field of the transmitted light to interact with the outer dielectric, as shown in Fig. 6. In order to fabricate an SPR based fiber-optic sensor, the silicon cladding from a small portion of the middle of the fiber was removed and the now unclad core was coated with different coating structures, such as a thin metal film for PSPR or metal nanoparticles for LSPR. These structures in turn were surrounded by a dielectric sensing layer (Jie et al., 2012).

4. The geometry of the optical fiber probe

In order to increase the sensitivity of the evanescent wave absorbance fiber-optic sensor, modification of the probe geometry was done (Sai et al., 2009). The typical probe designs include straight, U-bent, and tapered probe. The straight probe design is shown in Fig. 6. One drawback is its low penetration depth of the evanescent field ($<\lambda/10$)(Kundu et al., 2010),

which is far too small for sensing. Furthermore, the straight probe is unsuitable for larger analytes such as proteins and bacteria, since the dimension of bacteria and protein are about 1μm and 10 nm, respectively (Leung et al., 2007). Therefore, it is necessary to improve the penetration depth for sensing. The effects of bending and tapering on the evanescent field are discussed in this review.

4.1. The U-bent geometry

In a theoretical analysis of the two-dimensional U-bent sensor, the increase of its sensitivity is due to the variation of the angle of incidence. As shown in Fig. 7, the angle of incidence decreases along with the light rays propagating in the U-bent sensing region. Furthermore, the angle of incidence is related to the penetrating depth, which increases as the incident angle decreases. The bending of the optical fiber results in losing light and increasing the evanescent field. The advantages of choosing to use U-bent probes are their compactness, simplicity and their high sensitivity. Moreover, these U-bent tubes have a 10-fold improvement in absorbance sensitivity over straight probes (Sai et al., 2009).

In our previous studies, the fiber optic sensor was designed and constructed using a bent U-shape fiber optic probe to enhance absorbance (Duan et al., 2005; Duan et al., 2006; Zhao et al., 2011; Liang et al., 2015). In order to fabricate the U-bent fiber optic SPR sensor as shown in Fig. 7, firstly, the multi-mode fiber optic with a core diameter of 600 μm was cut to a length of 40 cm. The core was exposed in the middle of the fiber for a length of 4 cm with both ends of 1

cm. The jacket and the cladding on these sections were removed using a sharp surgical blade. To remove the revealed cladding, 50% HF was applied to the designated portion of the fiber for 10 min. Both ends of the fiber were polished by 5, 1, and 0.3 μm roughness emery papers in that order to enhance the intensity of the transmitted light. Finally, the core area in the middle was fabricated into a U-bend shape with the use of an alcohol blast burner, where the bend radius obtained was 0.35 cm (Liang et al., 2015). Then, the U-bent probe portion was coated with gold layer, these structures in turn were surrounded by a sensing medium layer.

The strength of the evanescent field is increased when the fiber is bent, thus increasing the sensitivity. A decrease of the bending radius also increases the sensitivity of the sensor. However, there is an optimal value of the sensitivity. Excessive bending of the fiber-optic probe results in a sharp decrease of its sensitivity. This results when the angle of incidence becomes less than the critical angle, which means that the condition of total reflection is not met. Furthermore, the sensitivity of the sensor increases as the sensing probe length increases within a given bending radius (Gupta and Verma, 2009).

4.2. Tapered probe

Other than the U-bent probe design, tapering the probe is also an effective method of improving the performance of the SPR based fiber-optic sensor. Fig. 8 illustrates the typical design of the tapered probe. A sensing probe of uniform core radius is sandwiched between two tapered fiber regions. Tapered region 1 decreases the angles of the bond rays in the fiber close to

the critical angle of the unclad tapered region, so all the rays are guided to the sensing region. Then these angles reconvert to their initial values in Region 2. Thus, the light rays propagate to the output end of the fiber. In order to avoid light ray leaks, the diameter of the sensing probe is minimized (Verma et al., 2007). The sensitivity is increased by tapering the fiber. Lower values of the angle of incidence guides more evanescent field into the region. Thus the coupling between the EW and the SPW is stronger. As shown in Fig.8, in sensing region, the evanescent electromagnetic field of EW excites the surface plasmons at the outer gold layer. When the wave-vector of the evanescent wave is equal to that of the surface plasmons, the resonance is generated. Lastly, the taper-shaped fiber optic sensor is fabricated. There are many reports about the elements which influence the sensitivity. The effects of taper ratio and taper profiles on the sensor's performance have been studied (Endo et al., 2005). Theoretical analysis predicted an increase in the sensitivity with an increase in the taper ratio. For example, a 5 times enhancement is realized for the taper ratio of 2.0 in comparison with the taper ratio of 1.0. Apart from the taper ratio, the taper profile can influence the performance of the sensor.

There are three taper profiles, exponential-linear, parabolic, and linear (Endo et al., 2005). The study reported by Rajneesh K. Verma showed that the exponential-linear taper profile with high taper ratio provided the best performance. It was reported that the fiber-optic SPR sensor was used for sensing vapor and liquid phase samples by tapering the probe (Verma et al., 2008).

4.3. Other probe designs

Other probe designs for SPR-based fiber-optic sensors have been reported (Wang et al., 2008; Kurihara et al., 2004; Gentleman and Booksh et al., 2006; Chiu et al. 2007; Hassani and Skorobogatiy, 2007; Lin et al., 2007). In the side-polished fiber sensor, two styles are involved, the single mode and the multimode fiber-optic sensors. The single-mode fiber-optic SPR sensor is more sensitive and accurate than the multimode fiber optic SPR sensor. However, the fabrication of the single-mode fiber optic sensor is more complex. A side-polished multimode fiber sensor based on SPR had been proposed by Yu Lin, et al. A halogen light was used as the light source and the side-polished multimode fiber-optic probe was used to detect the index liquid. The shift of the resonance wavelength was used as the signal variation, and the wavelength shift was dependent on the concentration of the test samples. The resolution of the wavelength interrogation was 3×10^{-6} refractive index units (RIU) (Kurihara et al., 2004). A single-mode D-shaped optic fiber was used in intensity measurements and phase measurements. There are four layers in a D-type SPR fiber sensor: the core, the cladding, SiO_2 and Au. The measured resolution of the intensity is in the range of 10^{-4} and 10^{-5}(RIU). An ideal incidence angle and an appropriate metallic thickness were chose to obtain a better sensitivity (Lin et al., 2007; Chiu and Shih, 2008). Furthermore, the dip-probe also improves the sensitivity of the SPR sensor. A method of manufacturing a robust dip-probe has been reported (Obando et al., 2004). Surface plasmons are excited in the region of the tip of the fiber-optic probe, which will increase the resolution (Abrahamyan and Nerkararyan, 2007). A photonic bandgap fiber-based SPR

sensor was also developed. The plasmon wave was excited by a leaky Gaussian-like core mode of a fiber (Gauvreau et al., 2007).

5. Applications of the fiber-optic SPR biosensor

Optical fiber biosensors are actively being pursued. These consist of a light source, an optical transmission medium (optical fiber), an immobilized biological recognition element and a physical transducer (Narsaiah et al., 2007). Using SPR in fiber-optic biosensing is based on the binding of the target analyte to the biological recognition element. The binding induces a variation in the refractive index of the absorbed layers at the metal surface (Marazuela et al., 2002). Thus the SPR coupling conditions are changed. The physical transducer converts the biorecognition event into a measurable optical or electric signal. These sensors possess the overall advantages of the fiber optic sensors. The inherent advantage of these sensors over traditional optical methods is a high sensitivity. Sub-femtomole levels of protein in complex fluids have been detected. Moreover, these fiber-optic biosensors were used to monitor binding kinetics.

Fiber-optic SPR biosensing is a portable, rapid, in-situ monitoring technology. Recently, researchers have paid more and more attention to its development and its applications. Biosensors are classified based on their immobilized biological recognition elements into immunosensors, DNA biosensors, enzyme biosensors and cell biosensors. All are affinity biosensors. They are described briefly below. The major applications of the SPR biosensor are

in the detection and identification of biological analytes and the analysis of biomolecular interactions (Homola et al., 2003). This section focuses on the detection of the biological analytes.

5.1. Immunoassay fiber-optic SPR biosensor

SPR based immunoassay has received extensive attention. An antibody or antibody fragment is used as a biorecognition element. When a surface immobilized antibody binds with an analyte within the range of the electric field (Shankaran et al., 2007), this binding perturbs the plasmon and changes the reflection intensity, which provides information about the concentration of the analyte. LSPR biosensor relies on the absorbance spectrum of a self-assembled monolayer of colloidal gold on the fiber optics. Since the optical properties of GNPs are sensitive to the refractive index of the surrounding medium, therefore, it is crucial to effectively immobilize the GNPs on the fiber surface. However, the lack of sufficient active groups on the surface of inorganic substrates such as fused silica restricts the quantity of the GNPs on the optical fiber. Therefore, effective methods are needed to generate enough anchoring points. In 2015, we reported a novel plasma enhanced U-bend fiber optic LSPR biosensor for label-free immunoassay for alpha-fetoprotein. The U-bend fiber optic probe was firstly pretreated by microwave-induced H_2O/Ar plasma to ensure better silanization, which could greatly improve the adsorbed amounts and uniformity of the gold nanoparticles (GNPs) on the fiber optic probe surface (Liang et al., 2015). Furthermore, on the basis of this U-bend strategy and plasma

pretreated method, the fabricated biosensor displayed good analytical performance for detection of AFP.

For large molecule antigens (Mr>2 kDa), their high mass is useful for sensitive sensing. They can be monitored in direct or sandwich formats. To achieve a high SNR and a low limit of detection, the affinity of the antibodies toward the target analytes must be large. The detection of the antibody of gamma–interferon showed that the sensitivity of the detector is also dependent on the optical system, the size of the particles and the effect of the gold nanoparticles (GNPs) aggregation (Jeong et al., 2011). However, using SPR in a small molecule immunoassay application is challenging. A simple summary of this problem is that the target small molecule antigen itself can't generate a sufficient SPR signal. Consequently, the antibody-antigen binding induces a small mass variation, which cannot provide a sensitive analysis. Thus, an application of the SPR immunoassay is focused on exploring the testing for small molecules. Direct detection of small molecule targets generally suffered from low signal and poor sensitivity. Hence, developing some suitable detection methods was needed.

Designing an appropriately functionalized sensor surface, utilizing the noble metal nanoparticles labels, and using suitable detection formats have been adopted in small molecule detection. To obtain high sensitivity, the assembly of the sensing surface was carefully considered. Carboxymethyl dextran polymers were commonly used to immobilize small molecule antigens to the gold surface. For instance, progesterone was immobilized on a dextran

surface by attaching an oligoethylene glycol (OEG) linker to the steroid (Mitchell et al., 2005). The appropriate linker chemistry protects the antigen and improves the binding signal, therefore, the sensitivity. In addition, suitable detection formats were used in small molecule detection. In 2010, John Mitchell et al. summarized the application of SPR technology to monitoring small molecules such as steroid hormones, toxins, drugs and explosives, in which they used a competitive SPR immunoassay to achieve signal enhancement and high sensitivity. The competitive immunosensor format refers to when the antigen is labeled with a high mass substance and used to compete with an unlabeled sample antigen for binding to the sensor surface. In general, gold nanoparticles and protein labels are used for signal enhancement. Recently, aptamers are potential alternatives to antibodies in small molecule SPR formats. Combining the advantages of aptamer technology with the amplifying effect of GNPs was used to provide a novel strategy for highly sensitive detection of adenosine. Potentially, a spectrum of target small molecules may be detected through immobilizing corresponding aptamers.

Miniaturized portable immunoassays devices play an important role in commercial success. The further development of SPR immunoassay systems will require significant advances in miniaturization of the SPR immunosensors. The on-site detection of low-molecular–weight analytes such as 2-hydroxybiphenyl (HBP) employing an indirect competitive format was achieved (Kim et al., 2006). The key of the monitoring was the use of the immunoreaction between the HBP-BSA conjugate and the anti-HBP antibody. The successful detection was based

on the changes in the resonance angle, since this is how the binding interaction between the HBP-BSA sensor chip and the anti-HBP antibody in the presence of free HBP was manifested. The detection limit was 0.1ng/ml, which was comparable with the conditional assays for the detection of HBP. In addition, the proposed immunosystem is promising for the online analysis of other small molecules. It should be possible to obtain wide applications of this model in biomedical, environmental and food safety analyses.

5.2. DNA fiber-optic SPR biosensors

Deoxyribonucleic acid (DNA) is a large molecule composed of four repeating subunits called nucleotides. The double helix structure of DNA is based on the base pairs adenine/thymine and cytosine/guanine. Internal hydrogen bonds hold the two strands of the DNA together. The double helix is broken apart by heat or a high pH. Moreover, a single stranded DNA (ss DNA) can hybridize to its complementary sequence (Zhai et al., 1997). The hybridization of DNA is measured with optical, electrochemical, or mass-sensitive devices (Sassolas et al., 2007). These methods are classified as a label or a label-free analysis. Label-based methods usually require tagging the analyte or ligand with enzymes, fluorescent dyes or metal nanoparticles. The labeling procedures are time-consuming. The labels themselves may interfere with the molecular interaction by blocking the active binding site. The labels may also cause suppression of the specific recognition ability of DNA-DNA hybridizations. The labels may also cause a high background signal (Ritzefeld and Sewald, 2012; Zhang et al., 2012). Therefore, a label-free and

low-cost analytical technique is urgently required.

Using SPR in sensing is based on the measurement of binding induced refractive index changes. SPR is a label-free optical method which detects DNA hybridization. Single-stranded DNA is usually immobilized on the probe surface. This strand will hybridize to the corresponding complementary strand if this exists in a test sample. This binding event on the gold layer disturbs the surface plasmons, therefore, the resonance conditions. The optical signals will change. In addition, the signal is proportional to the number of molecules. Therefore, some minimum number of DNA molecules is detected by fiber-optic LSPR biosensing (Zhai et al., 1997; Sassolas et al., 2007).

The most effective immobilizing process is affinity immobilization, which is normally achieved through a strong noncovalent biological interaction ($Ka=10^{15}M^{-1}$) (Ritzefeld and Sewald, 2012). Streptavidin is a tetrameric protein which has four identical binding sites for biotin, which is itself a small molecule (Zhang et al., 2012). The streptavidin is usually preimmobilized on the metal surface, to which it is covalently linked. Afterwards, the biotinylated single-stranded oligonucleotide probe is immobilized on the streptavidin-functionalized sensor surface.

Recently, fiber optic SPR DNA sensors have been used to explore DNA hybridization, DNA-protein interactions and peptide nucleic acid-DNA hybridization (Pollet et al., 2009; Endo et al., 2005). For DNA hybridization, the rapid detection of the invA gene to measure salmonella

was achieved by using the immobilized biotinylated probe. The invA sequence was recognized based on the biotin-streptavidin binding system, with a limit of detection of 0.5 nM (Zhang et al., 2012). The first research that combined the fiber-optic SPR system with DNA aptamer bioreceptors was reported by Jeroen Pollet et al. in 2009 (Pollet et al., 2009). Since then, the use of a protein-DNA interaction was reported by Ritzefeld et al. (Ritzefeld and Sewald, 2012). To evaluate the interaction of a protein with a nucleic acid, the ligand was immobilized on the sensor surface. Short biotinylated oligonucleotides were the most commonly used ligands. To effectively immobilize the ligands, the sensor surface was preimmobilized with streptavidin. Then the target protein analyte was injected into the fiber-optic SPR sample cell. Due to the formation of a protein-DNA complex, resulting in a variation of refractive index, sensing was accomplished by a change of wavelength. The concentration of protein molecules was proportional to the shift of the resonance wavelength. In addition, the fiber-optic LSPR DNA biosensor, based on peptide nucleic acid (PNA-DNA) hybridization, has also been reported (Endo et al., 2005). The PNA was immobilized on a gold-capped nanoparticle layer. The target DNA was recognized through the monitoring of the change of absorbance. Quantitative analysis of the target DNA (TNF-α), with a limit of detection of 0.677 pM, was achieved. PNAs are neutral, achiral DNA mimics, which possess some exceptional properties. The complexes of PNA with DNA or RNA sequences show higher thermal stabilities than DNA-DNA or DNA-RNA complexes. The other property of PNAs and their analogues is their resistance to

enzymes. The binding of the PNAs to the complementary DNAs has high affinity and specificity.

5.3. Enzyme fiber-optic SPR biosensor

Enzymes catalyze certain chemical reactions with high specificity. Enzyme biosensors usually utilize enzymes as the recognition elements. This has been an extensively studied area. For an enzyme fiber-optic SPR biosensor, the enzyme, such as glucose oxidase, was immobilized on the surface of a fiber-optic probe (Srivastava et al., 2012). When the functionalized probe was immersed into a glucose solution, the glucose was oxidized under the catalytic effect of the glucose oxidase.

$$\text{Glucose} + O_2 \xrightarrow{Glucose\,Oxidase} \text{Gluconic Acid} + H_2O_2$$

Due to the above reaction, the refractive index of the sensing region was changed, giving rise to a change in the SPR resonance condition. S.K. Srivastave and co-workers detected glucose in a flow cell having a straight fiber-optic probe. Wavelength modulation was used in this report and the wavelength shift was dependent on the concentration of the glucose. The obtained sensitivity was 0.036 nm/(mg/dl) (Srivastava et al., 2012). Afterwards, these workers used a U-shaped biosensor for the detection of blood glucose. The fast response and the small volume of the sensing sample (150 uL) promoted the development of the fiber-optic SPR based enzyme biosensor (Srivastava et al., 2012). Recently, the detection of organic compounds, especially pharmaceuticals have been paid more and more attention. Organic compounds such as acetylcholine (Chand et al., 2006), urea (Fujii et al., 2006), bilirubin (Choi et al., 2004) and

cholesterol (Choi et al., 2004) were monitored by immobilizing the corresponding enzyme on the surface of the fiber-optic SPR biosensors. More significantly, other targets are easily detected through using different enzymes.

5.4. Fiber-optic SPR living cell biosensor

Recently much attention has been paid to combining SPR technology with living cells. In general, the cell is immobilized on the gold layer/nanoparticles coated fiber-optic coupler. The external agent is injected to induce the cellular activity. The cellular morphology and the effective refractive index are varied simultaneously. The variation of the SPR signal is based on the changes of resonance angle for living cell reactions.

The difficulty of fixing the cell on the sensor chip is an experimental challenge, since the SPR is applied to respond to the events in the evanescent field. Some workers have reported measures to successfully solve this problem. Yuki Yanase et al. have developed methods of cell fixation and removal with HydroCell^{TM} or RepCell^{TM} (Yanase et al., 2007). Since then, a "droplet method" to easily fix either adherent or non-adherent cells on the tip of a fiber-optic sensor has been developed (Yanase et al., 2010).

Previous studies determined the receptor-mediated cellular signaling reactions (Ozawa et al., 1993; Kihara and Siraganian, 1994). Then, SPR based biosensing has been used to analyze ligand-induced cellular reactions (Hide et al., 2002). Significant SPR signals were emitted from living RBL-2H3 mast cells that had been stimulated by the antigen, dinitrophenol-human serum

albumin (DNP-HSA). More importantly, this report revealed that the SPR cell biosensors are able to detect the interactions between cells and biomolecules. Real-time monitoring of odorant-induced cellular reactions using SPR has also been demonstrated (Lee et al., 2009). OR17, an olfactory receptor, was expressed on the cell surface. The cells were human embryonic kidney (HEK)-293 cells. The binding of odorant molecules to the olfactory receptor generated the SPR signal. Among all the aldehydes tested, octanal resulted in the highest response signal due to the fact that it is the cognate odorant for the OR 17. The concentration of the odorant was proportional to the intensity of the SPR signal. Thus, the selective and quantitative detection of volatile compounds was achieved by the SPR sensing system, especially those compounds of environmental, health care, and pharmacological interest (Chabot et al., 2009). More interesting is that this portable SPR equipment appears to be important in the development of a biooptical nose.

In summary, all of the above four fiber-optic SPR biosensor rely on the measurement of binding-induced refractive index changes. Fiber-optic SPR biosensors are used extensively in some societally important sectors, such as medical diagnostics (Thanh and Rosenzweig 2002; Masson et al., 2004; Xu et al., 2011; Hong et al., 2012; Xu et al., 2012), environmental monitoring (Lin and Chung, 2008), and food safety and security (Slavík et al., 2002), which can govern the quality of life. Homola has reported the SPR based chemical sensors and biosensors. Herein, we have separately summarized examples of the use of the fiber-optic SPR biosensor for

the sensing of biochemical parameters in Table 2.

6. Conclusions

Recently the combination of the SPR phenomenon and fiber-optic technology has resulted in many advances in the sensing of chemical and biological species (Wolfbeis, 2000; Wolfbeis, 2002; Wolfbeis, 2004; Wolfbeis, 2006; Wolfbeis., 2008; Wang and Wolfbeis, 2013). Biological molecular recognition has been the object of most of this work. Since 1983, the SPR biosensors have been a competitive tool in analytical chemistry, bioanalysis, material science and surface science (Yonzon et al., 2004). However, we should note that the great majority of the applications in fields such as medical diagnostic have been on the monitoring of artificially buffered samples rather than real clinical samples. When using the SPR phenomenon in biosensing, a limit is the shallow penetration depth. The reactions are based on the surface of the probe, which is a challenge for researchers working to improve the sensor's specificity. Detecting specific molecules among groups of molecules and reducing the nonspecific interactions between sensor surface and unwanted molecules has been difficult. Nevertheless, the combination of SPR with optical fiber technology has brought significant advancements in both the probe designs of fiber-optic SPR sensors and the sensing of biochemical parameters. Future progress in this area will result in analytical systems capable of multi-analyte monitoring with good precision, acceptable stability, and finely tuneable specificity.

Acknowledgements

The authors acknowledge funding provided by the National Natural Science Foundation of China: Investigation of Fast Pathogen Detection Based on Novel Macroporous Chips Technology (no.21275105), National Recruitment Program of Global Experts (NRPGE) and the Hundred Talents Program of Sichuan Province (HTPSP), and the Startup Funding of Sichuan University for setting up the Research Center of Analytical Instrumentation. We also thank Jiantao, Tan and Guanghui Niu, for their assistances in the preparation of this article.

References

Abdulhalim, I.; Zourob, M.; Lakhtakia, A. Surface plasmon resonance for biosensing: a mini-review. *Electromagnetics* **2008**, *28*, 214-242.

Abrahamyan, T.; Nerkararyan, K.; Surface plasmon resonance on vicinity of gold-coated fiber tip. *Physics Letters A* **2007**, *364*, 494-496.

Chabot, V.; Cuerrier, C. M.; Escher, E.; Aimez, V.; Grandbois, M.; Charette, P. G. Biosensing based on surface plasmon resonance and living cells. *Biosens Bioelectron.* 2009, *24*,1667-1673.

Chen, Y.; Ming, H. Review of surface plasmon resonance and localized surface plasmon resonance sensor. *Phot. Sens.* **2012**, *2*, 37-49.

Chiu, M. H.; Shih, C. H. Searching for optimal sensitivity of single-mode D-type optical fiber sensor in the phase measurement. *Sens. Actuators, B,: Chemical* **2008**, *131*, 596-601.

Chiu, M. H.; Shih, C. H.; Chi, M. H. Optimum sensitivity of single-mode D-type optical fiber sensor in the intensity measurement. *Sens. Actuators, B,: Chemical* **2007**, *123*, 1120-1124.

Choi, M. M. F. Progress in enzyme-based biosensors using optical transducers. *Microchimica Acta* **2004**, *148*, 107-132.

Duan, Y. X.; Cao, W. Q. Optical fiber-based evanescent ammonia sensor. *Sens. Actuators, B,: Chemical* **2005**, *110*, 252-259.

Duan, Y. X.; Cao, W. Q. Optical fiber evanescent wave sensor for oxygen deficiency detection.

Sens. Actuators, B,: Chemical **2006**, 119,363-369.

Endo, T.; Yamamura, S.; Nagatani, N.; Morita, Y.; Takamura, Y.; Tamiya, E. Localized surface plasmon resonance based optical biosensor using surface modified nanoparticle layer for label-free monitoring of antigen–antibody reaction. *Science and Technology of Advanced Materials* **2005**, *6*, 491-500.

Endo, T.; Kerman, K.; Nagatani, N.; Takamura, Y.; Tamiya, E. Label-free detection of peptide nucleic acid-DNA hybridization using localized surface plasmon resonance based optical biosensor. *Anal. Chem.* **2005**, 77, 6976-6984.

Fujii, E.; Koike, T.; Nakamura, K.; Sasaki, S.i.; Kurihara, K.; Citterio, D.; Iwasaki, Y.; Niwa, O.; and Suzuki, K. Application of an Absorption-Based Surface Plasmon Resonance Principle to the Development of SPR Ammonium Ion and Enzyme Sensors. *Anal. Chem.*, **2002**, *74* 6106-6110.

Gauvreau, B.; Hassani, A.; Fehri, M. F.; Kabashin, A. Skorobogatiy, M. A. Photonic bandgap fiber-based Surface Plasmon Resonance sensors. *Opt. Express* **2007**, *15*, 11413-11426.

Gentleman, D. J.; Booksh, K. S. Determining salinity using a multimode fiber optic surface plasmon resonance dip-probe. *Talanta* **2006**, *68*, 504-515.

Guo, X. Surface plasmon resonance based biosensor technique: A review. *J. Biophotonics* **2012**, *5*, 483-501.

Gupta, B.; Verma, R. Surface plasmon resonance-based fiber optic sensors: principle, probe

designs, and some applications. *J. Sens*. **2009**, 979761-979773.

Hassani, A.; Skorobogatiy, M. Design criteria for microstructured-optical-fiber-based surface-plasmon-resonance sensors. *JOSA B* **2007**, *24*, 1423-1429.

Hide, M.; Tsutsui, T.; Sato, H.; Nishimura, T.; Morimoto, K.; Yamamoto, S.; Yoshizato, K. Real-time analysis of ligand-induced cell surface and intracellular reactions of living mast cells using a surface plasmon resonance-based biosensor. *Anal. Biochem.* **2002**, *302*, 28-37.

Homola, J. Surface plasmon resonance sensors for detection of chemical and biological species. *Chem. Revi.* **2008**, *108*, 462-493..

Homola, J. Present and future of surface plasmon resonance biosensors. *Anal. Bio. Chem* **2003**, *377*, 528-539.

Hong, Y.; Huh, Y. M.; Yoon, D. S.; Yang, J. Nanobiosensors Based on Localized Surface Plasmon Resonance for Biomarker Detection. *J. Nano.* **2012**, 759830-759843.

Jeong, H. H.; Erdene, N.; Lee, S. K.; Jeong, D. H.; Park J. H. Fabrication of fiber-optic localized surface plasmon resonance sensor and its application to detect antibody-antigen reaction of interferon-gamma. *Optical Engineering* **2011**, *50*, 124405-124405..

Jha, R.; Chand, S.; Gupta, B. D.; Surface Plasmon Resonance Based Fiber-Optic Sensor for Pesticide Detection. *Optical Society of America* **2006**, *240*, 6680-6685.

Jie, C.; Galbraith, E. K.; Tong, S.; Grattan, K. T. V. Cross-Comparison of Surface Plasmon Resonance-Based Optical Fiber Sensors With Different Coating Structures. *IEEE Sens. J.*

2012, *12*, 2355-23612361.

Kihara, H.; Siraganian, R. P. Src homology 2 domains of Syk and Lyn bind to tyrosine-phosphorylated subunits of the high affinity IgE receptor. *J. Biochem.* **1994**, *269*, 22427-22432.

Kim, S. J.; Gobi, K. V.,; Harada, R., D.; Shankaran, R.; Miura, N. Miniaturized portable surface plasmon resonance immunosensor applicable for on-site detection of low-molecular-weight analytes. *Sens. Actuators, B,: Chemical* **2006**, *115*, 349-356.

Kundu, T.; Sai, V. V. R.; Dutta, R.; Titas, S.; Kumar, P.; Mukherjee, S. Development of evanescent wave absorbance-based fibre-optic biosensor. *Pramana J. Phys.* **2010**, 75, 1099-1113.

Kurihara, K.; Ohkawa, H.; Iwasaki, Y.; Niwa, O.; Tobita, T.; Suzuki, K. Fiber-optic conical microsensors for surface plasmon resonance using chemically etched single-mode fiber. *Anal. Chim. Acta* **2004**, *523*, 165-170.

Lee, S. H.; Ko, H. J.; Park, T. H. Real-time monitoring of odorant-induced cellular reactions using surface plasmon resonance. *Biosens. Bioelectron.* **2009**, *25*,55-60.

Leung, A.; Shankar, P. M.; Mutharasan, R. A review of fiber-optic biosensors. *Sens. Actuators, B,*: Chemical **2007**, *125*, 688-703.

Liang, G.; Zhao, Z.; Wei, Y.,; Liu, K.; Hou, W.; Duan, Y. Plasma enhanced label-free immunoassay for alpha-fetoprotein based on a U-bend fiber-optic LSPR biosensor. *RSC*

Advances **2015**, *5*, 23990-23998.

Lin, H. Y.; Tsai, W. H.; Tsao, Y. C.; Sheu, B. C. Side-polished multimode fiber biosensor based on surface plasmon resonance with halogen light. *Applied Optics* **2007**, *46*, 800-806.

Lin, T. J.; Chung, M. F.; Using monoclonal antibody to determine lead ions with a localized surface plasmon resonance fiber-optic biosensor.*Sens.* **2008**, *8*, 582-593.

Marazuela, M. D.; Moreno-Bondi, M. C. Fiber-optic biosensors-an overview. *Anal. Bio. Chem.* **2002**, *372*, 664-682.

Marazuela, M.; Moreno-Bondi, M. Fiber-optic biosensors-an overview. *Anal. Bio.chem.* **2002**, *372*, 664-682.

Masson, J. F.; Obando, L.; Beaudoin, S.; Booksh, K. Sensitive and real-time fiber-optic-based surface plasmon resonance sensors for myoglobin and cardiac troponin. Talanta **2004**, *62*, 865-870.

Mayer, K. M. ; Hafner, J. H. *Localized surface plasmon resonance sensors*. *Chem. Revi.* **2011**, *111*, 828-3857.

Mitchell, J. S.; Wu, Y.; Cook, C. J.; Main, L. Sensitivity enhancement of surface plasmon resonance biosensing of small molecules. *Anal. Bio. Chem.* **2005**, *343*, 125-135.

Narsaiah, K.; Jha, S. N.; Bhardwaj, R.; Sharma, R.; Kumar, R. Optical biosensors for food quality and safety assurance—a review. *J. Food Sci.and Technol.* **2012**, *49*, 383-406.

Obando, L. A.; Gentleman, D. J.; Holloway, J. R.; Booksh, K. S. Manufacture of robust surface

plasmon resonance fiber optic based dip-probes. *Sens. Actuators, B,: Chemical* **2004**, *100*, 439-449.

Orellana, G.; Haigh, D. New trends in fiber-optic chemical and biological sensors. *Curr.Anal. C hem.* **2008**, *4*, 273-295.

Ozawa, K.; Yamada, K.; Kazanietz, M.; Blumberg, P.; Beaven, M. Different isozymes of protein kinase C mediate feedback inhibition of phospholipase C and stimulatory signals for exocytosis in rat RBL-2H3 cells. *J. Biochem.* **1993**, *268*, 2280-2283.

Piliarik, M.; Vaisocherova, H.; Homola, J. Surface plasmon resonance biosensing. *Methods in molecular biology* **2009**, *503*, 65-88.

Pollet, J.; Delport, F.; Janssen, K. P. F.; Jans, K.; Maes, G.; Pfeiffer, H.; Wevers, M.; Lammertyn, J. Fiber optic SPR biosensing of DNA hybridization and DNA–protein interactions. *Bios. Bioelectron.* **2009**, *25*, 864-869.

Ritzefeld, M.; Sewald, N. Real-Time Analysis of Specific Protein-DNA Interactions with Surface Plasmon Resonance. J. amino acids **2012**, 816032-816041.

Sai, V. V. R.; Kundu, T.; Mukherji, S. Novel U-bent fiber optic probe for localized surface plasmon resonance based biosensor. *Bios. Bioelectron.* **2009**, *24*, 2804-2809.

Sassolas, A.; Leca-Bouvier, B. D.; Blum, L. J. DNA Biosensors and Microarrays. *Chem.Rev.* **2007**, *108*, 109-139.

Shankaran, D. R.; Gobi, K. V.; Miura, N. Recent advancements in surface plasmon resonance

immunosensors for detection of small molecules of biomedical, food and environmental interest.*Sens. Actuators, B,: Chemical* **2007**, *121*, 158-177.

Sharma, A. K.,; Jha, R.; Gupta, B. Fiber-optic sensors based on surface plasmon resonance: a comprehensive review. *Sens. J. IEEE* **2009**, *7*, 979761-979773.

Slavík, R.; Homola, J.; Brynda, E. A miniature fiber optic surface plasmon resonance sensor for fast detection of staphylococcal enterotoxin B. *Biosens. Bioelectron.* **2002**, *17*, 591-595.

Srivastava, S. K.; Verma, R. K.; Gupta, B. D. Theoretical modeling of a localized surface plasmon resonance based intensity modulated fiber optic refractive index sensor. *Appl. opt.* **2009**, *48*, 3796-3802.

Srivastava, S. K.; Arora, V.; Sapra, S.; Gupta, B. D. Localized Surface Plasmon Resonance-Based Fiber Optic U-Shaped Biosensor for the Detection of Blood Glucose. *Plasmonics* **2012**, *7*, 261-268.

Srivastava, S. K.; Verma, R.; Gupta, B. D. Surface plasmon resonance based fiber optic glucose biosensor. *Proc. SPIE*, **2012**, *8351*, 83511Z-1.

Svedendahl, M.; Chen, S.; Dmitriev, A.; Kall, M. Refractometric Sensing Using Propagating versus Localized Surface Plasmons: A Direct Comparison. *Nano Letters* **2009**, *9*, 4428-4433.

Thanh, N. T. K.; Rosenzweig, Z.; Development of an aggregation-based immunoassay for anti-protein A using gold nanoparticles. *Anal.Chem.* **2002**, *74*, 1624-1628.

Verma, R.; Gupta, B. Theoretical modelling of a bi-dimensional U-shaped surface plasmon

resonance based fibre optic sensor for sensitivity enhancement. *J. Phys. D: Applied Physics* **2008**, *41*, 095106.

Verma, R. K.; Sharma, A. K.; Gupta, B. Surface plasmon resonance based tapered fiber optic sensor with different taper profiles. *Optics Communications* **2008**, *28*1, 1486-1491.

Verma, R. K.; Sharma, A. K.; Gupta, B. D. Modeling of tapered fiber-optic surface plasmon resonance sensor with enhanced sensitivity. *Photonics Technology Letters, IEEE* **2007**, *19*, 1786-1788.

Wang, X.; Wolfbeis, O. S., Fiber-optic chemical sensors and biosensors. Anal. Chem. **2013**, *85*, 487-508.

Wang, Y.; Qian, W.; Tan, Y.; Ding, S. A label-free biosensor based on gold nanoshell monolayers for monitoring biomolecular interactions in diluted whole blood. *Biosens. Bioelectron.* **2008**, *23*, 1166-1170.

Wijaya, E.; Lenaerts, C.; Maricot, S.; Hastanin, J.; Habraken, S., J.; Vilcot, P.; Boukherroub, R.; Szunerits, S. Surface plasmon resonance-based biosensors: From the development of different SPR structures to novel surface functionalization strategies. *Curr. Opin. in Solid Stat.and Materials Science* **2011**, *15*, 208-224.

Wolfbeis, O. S. Fiber-optic chemical sensors and biosensors. *Anal. Chem.* **2000**, *72*, 81R-89R.

Wolfbeis, O. S. Fiber-optic chemical sensors and biosensors. *Anal. Chem.* **2002**, *74*, 2663-2678.

Wolfbeis, O. S. Fiber-optic chemical sensors and biosensors. *Anal. Chem.* **2004,** *76*, 3269-3284.

Wolfbeis, O. S.; Fiber-optic chemical sensors and biosensors. *Anal. Chem.* **2006**, *78*, 3859-3874.

Wolfbeis, O. S.; Fiber-optic chemical sensors and biosensors. Anal. Chem. **2008**, *80*, 4269-4283.

Xu,X.; Ying, Y.; Li, Y. Gold Nanorods Based LSPR Biosensor for Label-Free Detection of Alpha-Fetoprotein. *Procedia Engineering* **2011**, *25*, 67-70.

Xu, X.; Ying, Y.; Li,Y. One-Step and Label-Free Detection of Alpha-Fetoprotein Based on Aggregation of Gold Nanorods. *Sens. Actuators B Chem.* **2012**, *175*, 194-200.

Yanase, Y.; Suzuki, H.; Tsutsui, T.; Uechi, I.; Hiragun, T.; Mihara, S.; Hide, M. Living cell positioning on the surface of gold film for SPR analysis. *Biosens. Bioelectron.* **2007**, *23*, 562-567.

Yanase, Y.; Araki, A.; Suzuki, H.; Tsutsui, T.; Kimura, T.; Okamoto, K.; Nakatani, T.; Hiragun, T.; Hide, M. Development of an optical fiber SPR sensor for living cell activation. *Biosens. Bioelectron.* **2010**, *25*, 1244-1247.

Yonzon, C. R.; Jeoungf, E.; Zou, S. L.; Schatz, G. C.; Mrksich, M.; Van Duyne, R. P. A comparative analysis of localized and propagating surface plasmon resonance sensors: The binding of concanavalin a to a monosaccharide functionalized self-assembled monolayer. *J. ACS.* **2004**. *126*, 12669-12676.

Zhang, D.; Yan, Y.; Li, Q.; Yu, T.; Cheng, W.; Wang, L.; Ju, H.. Ding, S. Label-free and high-sensitive detection of Salmonella using a surface plasmon resonance DNA-based biosensor. *J. Biotechnology* **2012**, *160*, 123-128.

Zhai, J.; Cui, H.; Yang, R. DNA based biosensors. *Biotechnology advances* **1997**, *15*, 43-58.

Zhao, J.; Zhang, X.; Yonzon, C. R.; Haes, A. J.; Van Duyne, R. P. Localized surface plasmon resonance biosensors *Nanomedicine* **2006**, *1*, 219-228.

Zhao, Z.; Duan, Y. A low cost fiber-optic humidity sensor based on silica sol–gel film. *Sens. Actuators, B,: Chemical* **2011**, *160*, 1340-1345.

Table 1. Comparision of LSPR and SPR. Reprinted with permission from (Homola et al., 2008). Copyright (2008) American Chemical Society.

	LSPR	SPR
Bulk dielectric sensitivity (nm/RIU)	10^2	10^6
sensing distance(nm)	10	1000
temperature sensitive?	no	yes
simple instrumentation?	yes	no

Table 2 Overview of the application of the fiber-optic SPR biosensors

Analyte	technique	biosensor	detection format	LOD/sensitivity	References
HBP	SPR	immunoassay	competitive	0.1ng/mL (ppb)	Kim et al., 2006
IgG	LSPR	immunoassay	direct	0.8nM	Kund et al., 2009
Lead(Ⅱ)	LSPR	immunoassay	direct	0.27ppb	Lin et al., 2008
Cadmium	LSPR	immunoassay	direct	0.16ppb	Lin et al., 2009
SEB	SPR	immunoassay	sandwich	0.5ng/mL	Chau et al., 2006
CEA	SPR	immunoassay	direct	0.5ng/mL	Tang et al., 2006
Fibrinogen	LSPR	immunoassay	direct	10ng/mL	Endo et al.,2005
AFP	LSPR	immunoassay	direct	0.25nM	Xu et al., 2011
Interleukin-1β	LSPR	immunoassay	direct	21pg/mL	Chiang et al., 2010
Salmonella	SPR	DNA		0.5nM	Zhang et al., 2012
Human IgE	SPR	DNA		2nM	Pollet et al., 2009
TNF-α	SPR	DNA		0.677pM	Endo et al., 2005
Urea	SPR	enzyme		10^{-4}-10^{-1} M	Fujii et al., 2002
Glucose	LSPR	enzyme		0.036nm/mg/dl	Srivastava et

			al.2012
Pesticide	SPR	enzyme	Jha et al., 2006
RBL-2H3	SPR	cell	Yanase et al., 2010
peripheral B	SPR	cell	Yanase et al.,2007
DNP-HSA	SPR	cell	Hide et al., 2002
(HEK)-293	SPR	cell	Lee et al., 2009

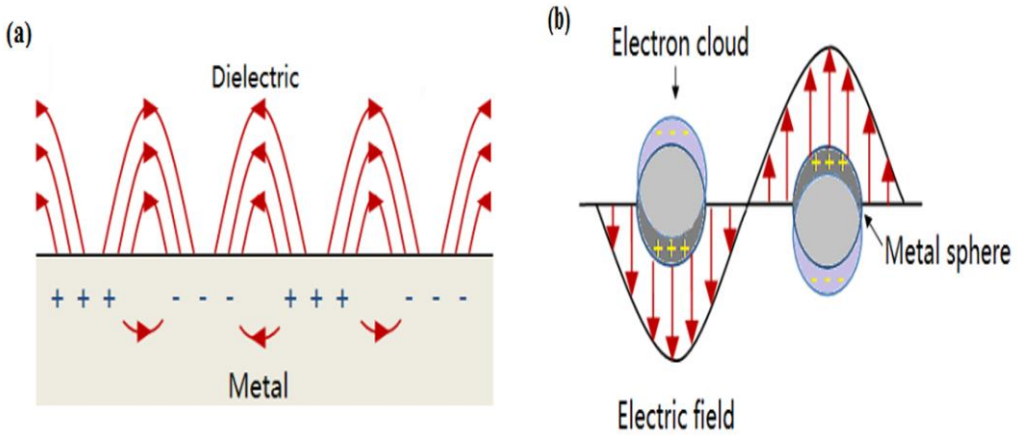

Fig. 1. Illustrations of (a) surface plasmon (in the planar metal film) (b) localized surface plasmon (in the metallic nanostructures). Reprinted with permission from (Guo et al., 2012). Copyright (2012) Wiley Online Library.

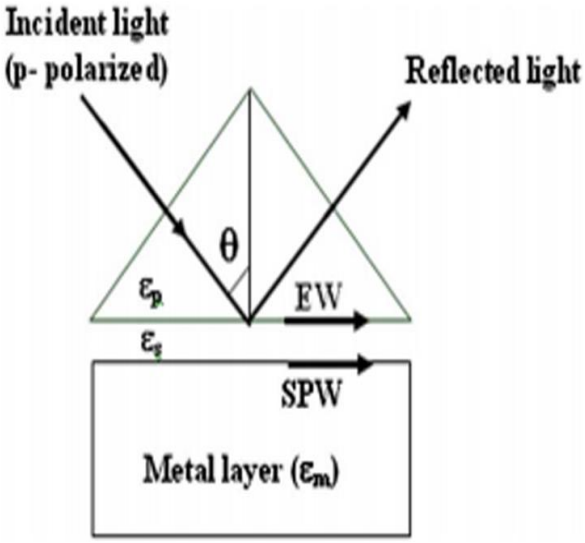

Fig. 2. Otto configuration. Reprinted with permission from (Sharma et al., 2009). Copyright (2009) IEEE.

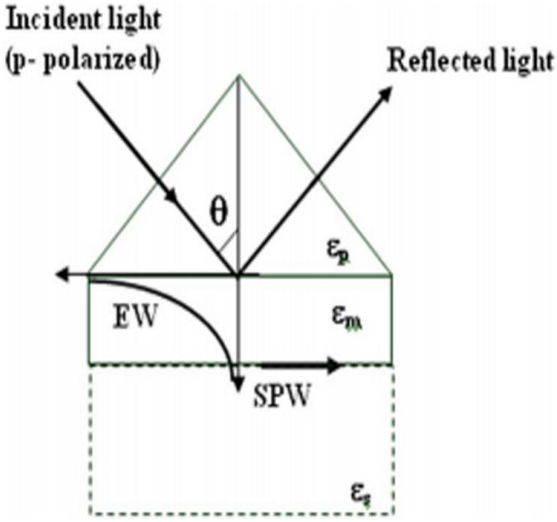

Fig. 3. Kretschmann configuration. Reprinted with permission from (Sharma et al., 2009). Copyright (2009) IEEE.

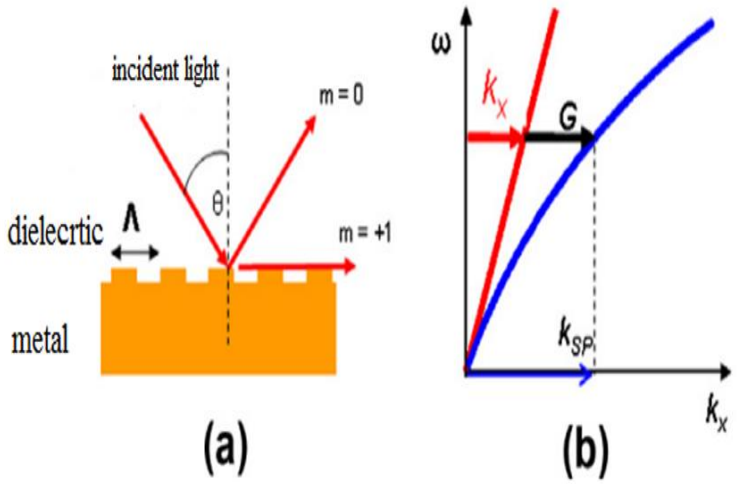

Fig. 4. (a) Excitation of surface plasmons by a diffraction grating (b) Dispersion diagram illustrating the phase-matching condition. The component along the x-axis of the incident light, k_x is increased by G to match the associated surface plasmons. Reprinted with permission from (Wijaya et al., 2011). Copyright (2011) Elservier.

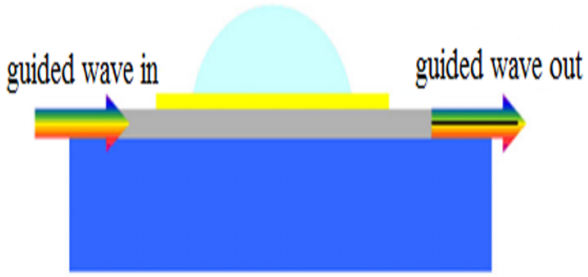

Fig. 5. Excitation of surface plasmons by waveguide coupling. The dark blue layer indicates the substrate, the gray layer indicates the waveguide, the yellow layer indicates the metal film, and the light blue layer indicates the dielectric. Reprinted with permission from (Wijaya et al., 2011). Copy right (2011) Elservier.

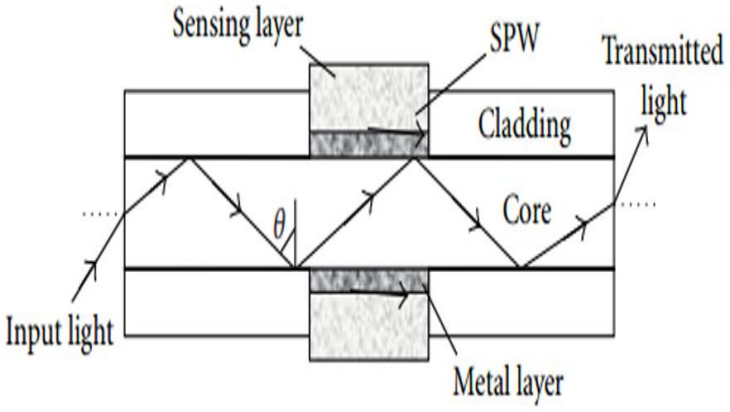

Fig. 6 Illustration of a typical fiber-optic SPR sensor. Reprinted with permission from (Verma et al., 2008). Copyright (2008) IOP Science.

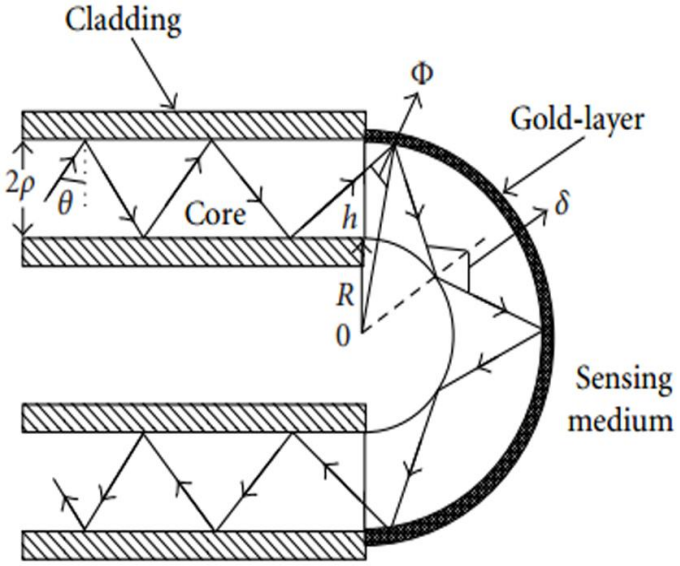

Fig. 7 U-bent fiber-optic SPR probe. Reprinted with permission from (Verma et al., 2008). Copyright (2007) IOP Science.

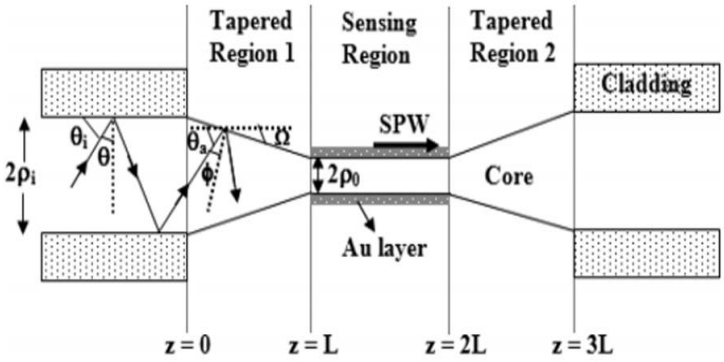

Fig. 8 Tapered fiber-optic SPR probe. Reprinted with permission from (Verma et al., 2007). Copyright (2007) IEEE.